Symbolic dynamics and the discrete variational principle

1998 J. Phys. A: Math. Gen. 31 9065

(http://iopscience.iop.org/0305-4470/31/45/006)

J. Phys. A: Math. Gen. **31** (1998) 9065–9072. Printed in the UK PII: S0305-4470(98)92740-8

Symbolic dynamics and the discrete variational principle

H R Dullin

Department of Applied Mathematics, University of Colorado, Boulder, USA and Institut für Theoretische Physik, Universität Bremen, Germany

Received 24 March 1998, in final form 14 August 1998

Abstract. We show how to construct symbolic dynamics for the class of $2d$-dimensional twist mappings generated by piecewise strictly convex/concave generating functions. The method is constructive and gives an efficient way to find all periodic orbits of these high-dimensional symplectic mappings. It is illustrated with the cardioid and the stadium billiard.

1. Introduction

By a dictum of Poincaré, periodic orbits are 'the only breach through which we may attempt to penetrate an area hitherto deemed inaccessible' [1]. Today this is a well established fact in the theory of dynamical systems. Classical global characteristic properties like Lyapunov exponents or diffusion coefficients are calculated by sums over periodic orbits [2, 3]. Particularly interesting is the fact that quantum mechanical properties can also be revealed by summation over classical periodic orbits [4, 5]. This has stimulated renewed interest in classifying and calculating periodic orbits [6–8].

Symbolic dynamics uniquely labels all orbits of a dynamical system by bi-infinite sequences [3]. The advantage of the variational approach to symbolic dynamics is nicely illustrated by labelling periodic geodesics of geodesic *flows* on the torus or on surfaces with higher genus as follows. Wind a string around the surface in an arbitrary way. The variational principle states that pulling the string tight to its shortest possible length yields a geodesic of the system by the stationarity of the length, respectively action. Winding the string in a topologically different way gives a different geodesic. The topologically different closed paths of a surface are classified by the fundamental group of the surface, so that the distinct words from the fundamental group label distinct geodesics of the surface.

We present an analogous result for *maps* which yields their symbolic dynamics and a method to calculate all orbits. We follow the variational approach to symplectic maps [9–11]. For an introduction to the two-dimensional case see [12], for $2d$-dimensional maps, $d \geqslant 2$, see [13, 14]. Our arguments hold for arbitrary d and since the global topology of configuration space does not enter our considerations, we just assume $x, x' \in \mathbb{R}^d$. The calculation is formulated in a way that makes it almost independent of d. The Lagrangian $L(x, x')$ acts as the generating function (of Goldstein type 1) for the map $(x', y') = F(x, y)$. The symplectic map F is implicitly defined by

$$y = -\frac{\partial L}{\partial x} =: -L_1(x, x') \qquad y' = \frac{\partial L}{\partial x'} =: L_2(x, x') \tag{1}$$

where the twist condition $\det L_{12} \neq 0$ must be fulfilled. L_{ij} denotes the matrix of partial derivatives with respect to the ith and the jth argument. The mapping from (x, x') to

$(x, y) = (x, -L_1)$ is the discrete analogue of the Legendre transformation. The periodic action of a sequence $\boldsymbol{x} = (x_1, \ldots, x_n)$ is given by

$$W_n(\boldsymbol{x}) = \sum_{i=1}^{n} L(x_i, x_{i+1})\Big|_{x_{n+1}=x_1}. \tag{2}$$

The variational principle states that the critical points $\boldsymbol{x}^*$ of the action W_n, for which $\nabla W_n(\boldsymbol{x}^*) = 0$, correspond to the physical orbits of the system. For period-n orbits we explicitly obtain

$$\frac{\partial W_n(\boldsymbol{x})}{\partial x_i} = L_2(x_{i-1}, x_i) + L_1(x_i, x_{i+1}) = 0 \tag{3}$$

for $i = 1, \ldots, n$. For twist maps of $\mathbb{T}^d$ the boundary conditions are altered to $x_{n+1} = x_1 + m$ with $m \in \mathbb{Z}^d$. In summary, the problem of classifying and calculating period-n orbits of the map F is equivalent to the problem of classifying and calculating the critical points of W_n.

Classifying and calculating *all* critical points of a function of nd variables is a formidable problem in general. We will single out a class of generating functions L for which it can be solved. For this class of systems our method gives a symbolic dynamics and simultaneously a numerical method to find all periodic orbits. The approach is based on the assumption that L is piecewise strictly convex or concave. We call a map obtained from such a generating function *piecewise strictly convex/concave twist maps*, or CTM. Our arguments hold for both convex and concave generating functions, but we will only state them for the convex case. The concave case is obtained by replacing L by $-L$. Note that a convex L corresponds to a dispersing billiard, while a concave L corresponds to a focusing billiard. In the former the action of periodic orbits is maximal, while in the latter the action is minimal.

Finding periodic orbits in Lagrangian twist maps respectively billiards by extremizing the action is a well known method. In the general case it is necessary to find critical points of arbitrary index, which is numerically done by finding the zeroes of the gradient of the action. For CTMs this is not necessary and more efficient methods (e.g. conjugate gradients) can be used for finding minima/maxima of the action.

Bunimovich's treatment of 3D dispersing billiards [15] like the Sinai billiard was an essential inspiration for this paper. Earlier work in this direction treated 2D dispersing billiards [16–18]. Even though Bunimovich treats special 2D focusing billiards in [15], the proof is not based on properties of the action but rather 'on some general properties of hyperbolic billiards'. Our approach shows that it actually is possible to also treat focusing billiards with the variational approach. This is particularly interesting because it gives a method that can be used to treat focusing billiards in higher dimensions.

2. Piecewise strictly convex twist maps

By definition of convexity the Lagrangian L is strictly convex in a subdomain U if

$$L(tu + (1-t)v, tu' + (1-t)v') < tL(u, u') + (1-t)L(v, v') \tag{4}$$

for all $(u, u'), (v, v') \in U \subset \mathbb{R}^{2d}$ and $t \in (0, 1)$, see e.g. [19]. If L is twice differentiable in this subdomain then convexity is equivalent to the Hessian of L

$$D^2L(x_i, x_{i+1}) = \begin{pmatrix} L_{11}(x_i, x_{i+1}) & L_{12}(x_i, x_{i+1}) \\ L_{21}(x_i, x_{i+1}) & L_{22}(x_i, x_{i+1}) \end{pmatrix} \tag{5}$$

being positive definite on the subdomain U. Note that we require L to be piecewise convex as a function of both variables, as opposed to requiring either the kinetic part of L or its twist to be convex.

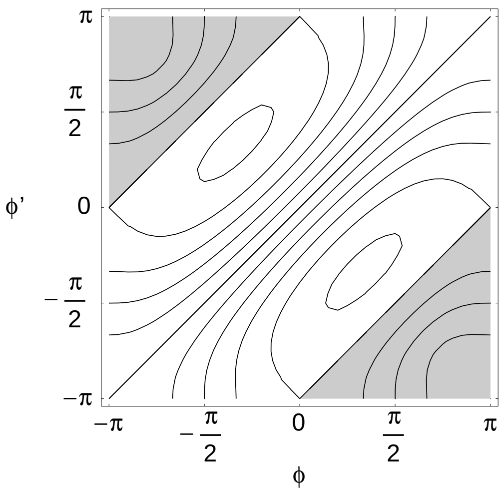

Figure 1. Contour plot of the generating function $L(\phi, \phi')$ for the cardioid billiard. The function has $N = 2$ smooth concave twisting regions U_i surrounding the two maxima. Regions of non-physical orbits are grey.

We always assume that the twist condition $\det L_{12} \neq 0$ holds. For CTMs we additionally require that the domain of L can be covered by subdomains U_i such that L restricted to each U_i is strictly convex, as e.g. shown in figure 1. Note that this implies that L is not differentiable at the boundary of the subdomains U_i. However, the singular set $\gamma = \bigcup_i \partial U_i$ has zero measure. The singularity of L induces a singularity for the action (2) on the set $\Gamma = \{\boldsymbol{x} : (x_j, x_{j+1}) \in \gamma\}$. Each U_i is called a *smooth convex twisting* region. Our arguments hold for both convex and concave generating functions, but we will only state them for the convex case.

The essential observation is that the piecewise strict convexity of L implies the piecewise strict convexity of W_n. Since a strictly convex function has at most one minimum, we can picture the action as a relief solely composed of nd-dimensional paraboloid-shaped patches. The place where patches meet corresponds to the singularity Γ. True paraboloids would correspond to a quadratic Lagrangian, hence a linear map. The convexity argument generalizes this to the nonlinear case. By convexity there is a simple superposition principle for the functions L, although they might be highly nonlinear. Take any two points $\boldsymbol{u} = (u_1, \ldots, u_n)$ and $\boldsymbol{v} = (v_1, \ldots, v_n)$ from $\mathbb{R}^{nd}$ such that the straight line connecting them does not cross the singularity Γ. The strict convexity of W_n on the singularity-free region containing $\boldsymbol{u}$ and $\boldsymbol{v}$ means that

$$W_n(t\boldsymbol{u} + (1-t)\boldsymbol{v}) < tW_n(\boldsymbol{u}) + (1-t)W_n(\boldsymbol{v}). \tag{6}$$

This is true because by (4) every single term in (2) is bounded from above. Again assuming L to be twice differentiable on each subdomain U_i we can alternatively prove the strict convexity of W_n by showing that the Hessian D^2W_n of W_n is positive definite everywhere outside the singularity set Γ. By definition this means that $\boldsymbol{z}^t D^2 W_n \boldsymbol{z} > 0$ for all $\boldsymbol{z} = (z_1, \ldots, z_n) \neq 0$, $z_i \in \mathbb{R}^d$. Explicitly we find

$$\boldsymbol{z}^t D^2 W_n(\boldsymbol{x})\boldsymbol{z} = \sum_{i=1}^{n} \begin{pmatrix} z_i \\ z_{i+1} \end{pmatrix}^t D^2 L(x_i, x_{i+1}) \begin{pmatrix} z_i \\ z_{i+1} \end{pmatrix} \tag{7}$$

with periodic boundary conditions on x and z understood. By assumption that $D^2L > 0$ each term in the sum is positive definite, such that D^2W_n is positive definite. Note that D^2W_n is not block diagonal, but instead the matrices $D^2L(x_i, x_{i+1})$ partially overlap. We now use the fact that W_n is piecewise strictly convex to construct symbolic dynamics.

3. Symbolic dynamics

Consider the sets U_j, $j = 1, \ldots, N$ on which L is smooth convex twisting. Typically each U_j contains a non-degenerate minimum of L. Now we try to construct a periodic orbit $\boldsymbol{x}$ with period n that first visits U_{j_1} then U_{j_2} etc, in general $(x_i, x_{i+1}) \in U_{j_i}$. We denote the corresponding region in $\mathbb{R}^{nd}$ by $U(J)$, where the sequence

$$J = \{j_1, j_2, \ldots, j_n\} \qquad 1 \leqslant j_i \leqslant N \tag{8}$$

will be a word in the symbolic dynamics with letters $1, \ldots, N$. Its infinite repetition labels the periodic orbit in question. Every sequence J corresponds to a region $U(J)$ in which W_n is strictly convex. If $\boldsymbol{x} \in \partial U(J)$ then it is in the singular set Γ. Since there are N regions in L, there are N^n different sequences J of length n, and therefore there are N^n disjoint regions $U(J)$ of piecewise convexity of W_n. Every period-n orbit of the map F induces n critical points of W_n, corresponding to the cyclic permutations of its points. We have shown that all critical points are minima. Every minimum is contained in a convex region, therefore it can be uniquely labelled by a sequence J. Up to a cyclic permutation of the indices in J the periodic orbit is therefore uniquely labelled, and we have found a symbolic dynamics for the map F. The standard approach to symbolic dynamics is via a partition of the phase space of F. We can lift our partition from the space of (x, x') to the phase space of the map with coordinates (x, y) using the Legendre transformation (1). The result is a partition of phase space which will have singularities as its boundaries, cf the $d = 1$ approach in [20].

Every periodic orbit can be labelled by a sequence J. However, not every sequence corresponds to a (physical) orbit. This phenomenon is called pruning. There are two ways in which pruning comes about in our setting. (For billiards it is often convenient to work with an artificially enlarged definition range for L, which introduces a third pruning mechanism.) First, the set $U(J)$ might be empty, in which case J and all the words containing J do not correspond to orbits. We call this *intrinsic pruning*, since it only depends on the geometry of the partition U_j. Secondly, the minimum that by convexity is guaranteed to exist in $U(J)$ [19] might be attained on the boundary $\partial U(J)$. We call this *extrinsic pruning*, since it depends on the properties of the action W_n. In the linear case we would have a patch of a parabola which does not include its minimum. So in order to prove that any of the N^n orbits exist, it is necessary to show that $U(J)$ is non-empty and that the gradient of W_n is pointing into $U(J)$ on the boundary $\partial U(J)$. In any case, $\ln N$ is an upper bound on the topological entropy of F, extending the result of [16] to focusing billiards whose Poincaré map is a CTM. If every minimum exists there are N^n fixed points of the n-times iterated map, so that the topological entropy cannot exceed n.

4. Finding periodic orbits

Using the gradient flow of W_n to find critical points is a well known idea. It is particularly powerful in the present case because we can show that W_n is piecewise strictly convex, hence we know that *all* critical points of W_n are local minima. The hard part in finding *all* critical points of a function usually is finding the saddle points, which do not exist in our case. Note that for $d = 1$ this means that there are no inverse hyperbolic orbits, because by a formula of [21] they correspond to saddles of W_n. Placing an initial condition $\boldsymbol{x}(0)$ into any of the convex pieces $U(J)$ of W_n and integrating the flow

$$\dot{\boldsymbol{x}} = \nabla W_n(\boldsymbol{x}) \qquad \boldsymbol{x}(0) \in U(J) \tag{9}$$

will either converge to the local minimum, i.e. the critical point with label J, or, if there is no minimum in $U(J)$, the flow will hit the singularity. In practice a different minimum-finder that is more efficient than integrating the gradient flow would be used, see [22]. Note that for the action of a non-CTM one has to use root-finding methods for the gradient, typically Newton's method, to locate critical points. But it is numerically much simpler to find minima [22]. Therefore in our case the use of Newton's method is discouraged, except possibly for 'polishing' the solutions. We have now achieved the complete classification of the basins of attraction of all the critical points. Under the gradient flow ∇W_n the set $U(J)$ is attracted to the critical point J, if it exists. Not only have we turned the problem of calculating unstable periodic orbits into a stable numerical procedure, but we have also simplified the problem of choosing the initial condition such that it converges to any desired periodic orbit. The latter is the main practical problem that prevents standard methods from finding *all* orbits efficiently.

Given a J it might not be easy to find an $\boldsymbol{x}(0)$ in $U(J)$. As we have already pointed out, $U(J)$ might even be empty. Concerning this intrinsic pruning one can construct the forbidden words J by the following procedure. The letter j can be followed by the letter k if the set U_k is reachable from the set U_j. Denote the projections of a set U onto the coordinate plane x' by $\pi'(U)$. Now define $U_j \wedge U_k$ as the subset of U_k that is reachable from U_j,

$$U_j \wedge U_k = \{(x, x') \in U_k : x \in \pi'(U_j)\}. \tag{10}$$

Thus j can be followed by k iff $U_j \wedge U_k \neq \emptyset$. The procedure can be refined by looking at $(U_j \wedge U_k) \wedge U_l$ etc, possibly yielding longer and longer intrinsically pruned words. Similar considerations apply for backwards time.

In the sense mentioned in the introduction, fixing J only fixes the topology of the periodic orbit. For a geodesic flow on a surface the topologically different paths are not deformable into each other, because the topology of the surface prevents it. In our case the situation is not so 'clean', because it is only the singularity that prevents the deformation of one orbit into another one. However, we have reached a surprising level of conceptual similarity to the case of geodesic flows by employing the discrete variational principle.

5. Application

One might think that the conditions placed on L are very restrictive, and with all the singularities involved there are only exceptional dynamical systems that fulfil them. This is correct—the conditions imply that a CTM is strongly chaotic in the sense of d non-vanishing Lyapunov exponent for almost every initial condition, as will be shown in a forthcoming paper. Such maps are the exception. Thus, the examples are prominent ergodic systems: the dispersing Sinai billiard in three dimensions was treated in [15]; here we treat the cardioid and the stadium billiard as examples of the focusing case.

5.1. Cardioid billiard

The cardioid billiard was introduced in [23] and shown to have non-vanishing Lyapunov exponent in [24]. The symbolic dynamics was introduced in [25, 26]. The above general considerations prove that this symbolic dynamics and the numerical method used in [25] are valid. For billiards the generating function reads $L(s, s') = |r(s) - r(s')|$, where s is the arc length of the billiard boundary and $r(s)$ is the corresponding point on the boundary. The contour plot of this function using polar coordinates for the cardioid $\rho(\phi) = 1 + \cos\phi$

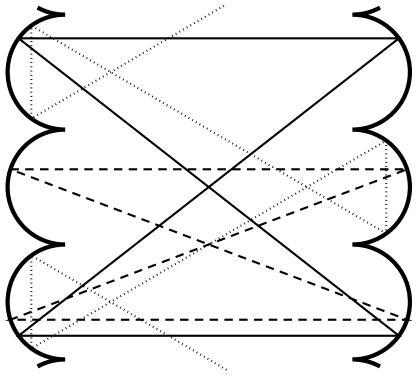

Figure 2. The periodic stadium billiard, which has a piecewise concave generating function. Three orbits of period 8 (full), 3 (broken), and 6 (dotted) in the stadium billiard with period 4 (code 002000-20), 4 (code 001000-10) and ∞ (code 111-1) in the periodic stadium billiard, respectively.

is shown in figure 1. For billiards inside subdomains of $\mathbb{R}^2$ the twist is positive, and the orbits we are studying are maxima of W_n. Since for billiards $L(s, s') = L(s', s)$, figure 1 clearly shows the two maxima of W_2 corresponding to one period-two orbit.

By a calculation similar to the one in [25] it can be shown that for the cardioid L is piecewise concave with $N = 2$ pieces. Intrinsic pruning does not exist for this system, we even have $U_j \wedge U_k = U_k$. Besides some extrinsic pruning (called 's-pruning' in [25]), the most important pruning mechanism comes about by considering L as a function of the full square in figure 1, as opposed to restricting it to the physical non-shaded region. This is related to the fact that the billiard is not convex, and not every line connecting $r(s)$ and $r(s')$ is completely inside the billiard. However, the generating function is blind to the fact that the connecting line intersects the billiard boundary. One could restrict the definition of L to the non-shaded area of physical orbits in figure 1. From a practical point of view it is more convenient to ignore this restriction, and find all periodic orbits, regardless of whether they are physically forbidden or not. In a second step it is then decided if they are valid or not, i.e. if they have a point (ϕ_i, ϕ_{i+1}) in the shaded region.

5.2. *Stadium billiards*

The stadium billiard of Bunimovich [27] has been well studied. We propose a new method to classify and calculate its periodic orbits. The method proposed in [28] also uses a flow, but it is different from ours. By the above reasoning it is proven that our symbolic dynamics and the accompanying numerical method works if we can show that L is piecewise convex. For this consider the 'unfolding' of the stadium billiard into a billiard which is partially unbounded and periodic, see figure 2. Alternatively, it could be defined on a cylinder.

In order to show that our method applies we have to analyse the generating function L between two half-circles of radius normalized to 1 with centres segregated by $(n\Delta_x, m\Delta_y)$, which is given by

$$L^{(n,m)}(s, s') = \sqrt{(\cos s - \cos s' - n\Delta_x)^2 + (\sin s - \sin s' - m\Delta_y)^2} \qquad (11)$$

where $\Delta_y = 2r$. If s and s' are unrestricted, L is a function on $\mathbb{T}^2$ with a quite complicated structure. But we restrict to the half-circles facing each other as in figure 2, starting on the right, $-\pi/2 < s < \pi/2$, ending on the left, $\pi/2 < s' < 3\pi/2$, and therefore $n\Delta_x < 0$. Now we are going to show that L is concave in the physical region, i.e. where a line has exactly one intersection with each half-circle. With the notation

$$A = 1 - \cos(s - s')$$

$$B = n\Delta_x \cos s + m\Delta_y \sin s$$
$$C = n\Delta_x \cos s' + m\Delta_y \sin s'$$

we can write

$$L^2 = n^2\Delta_x^2 + m^2\Delta_y^2 - 2(B - C) + 2A \tag{12}$$

and the Hessian is

$$\frac{1}{L^3}\begin{pmatrix} (B-A)(L^2+(B-A)) & -(-C-A)(B-A) \\ -(-C-A)(B-A) & (-C-A)(L^2+(-C-A)) \end{pmatrix}. \tag{13}$$

For the ray connecting the centres of the circles the Hessian is always negative definite. Since a Hessian is symmetric the determinant must vanish in order to lose negative definiteness. The determinant is given by

$$\frac{1}{L^4}(B-A)(-C-A)(n^2\Delta_x^2 + m^2\Delta_y^2 - (B-C)). \tag{14}$$

The first two non-trivial factors are zero if the orbit is tangent to a circle. But a tangency is only possible outside the physical region. The third factor is always non-zero in the physical region because it is the projection of the orbit segment onto $(n\Delta_x, m\Delta_y)$. Therefore (11) is concave in the physical region. The concave region even extends into the non-physical region up to the point of tangency on either half-circle (if it exists). If the chosen minimum-finder always decreases the function value (like the gradient flow would) one can extend the half-circles to full circles. This is convenient because the boundary conditions need not be checked. Moreover, as soon as the minimum-finder leaves the half-circles one can conclude that the corresponding orbit is pruned. The initial condition must of course connect the half-circles. By extending the half-circles to full circles the singularity can be removed, so that it does not pose any problem in the numerics.

An arbitrary number c of reflections within one and the same half-circle can be subsumed in the generating function

$$L^{(c)}(s_1, s_c) = 2c \sin\frac{s_c - s_1}{2|c|}. \tag{15}$$

In order to introduce a coding, we number the half-circles according to their horizontal position by r_i and l_i for the right and left row, respectively. Now we start e.g. on the right at r_0, next hit l_1, make a number c_1 of reflections within l_1, either clockwise ($c_1 < 0$) or anticlockwise ($c_1 > 0$); then continue to r_2 etc. The important quantities are the differences $\Delta_1^l = l_1 - r_0$, $\Delta_2^r = r_2 - l_1$ etc, where the upper index denotes motion to the left or right. Thus we form sequences $\Delta_1^l c_1 \Delta_2^r c_2 \Delta_3^l c_3 \ldots$, where each entry is in $\mathbb{Z}$, see figure 2 for some examples. The period in the reduced stadium is the sum of the absolute values of these integers. An inverse hyperbolic orbit of the stadium appears as a direct hyperbolic orbit with doubled period in the periodic stadium (e.g. the broken-line orbit). These orbits have an odd number of reflections with the vertical walls. If the number of reflections with both the upper and lower vertical wall is odd, the orbit becomes unbounded in the periodic stadium. In this case we have to change the periodic boundary conditions to $x_{n+1} = x_1 + \sum \Delta_i$. For the period-6 orbit in figure 2 the periodic action W_6 reads

$$W_6(s_1, s_3, s_4, s_6) = L^{(-1,-1)}(s_1, s_3) + L^{(1)}(s_3, s_4) + L^{(1,-1)}(s_4, s_6) + L^{(-1)}(s_6, s_1). \tag{16}$$

One technicality remains because the generating function for reflections within one circle (15) is only concave, rather than strictly concave, as must be the case for an integrable system. The non-zero kernel of D^2L accounts for the fact that most periodic orbits of an integrable system are not isolated, but come in families forming tori. But note that each appearance of the circle-generating function (15) in the action (2) and similarly in (7) is preceded and followed by the strictly concave generating function between two half-circles (11). Hence even if we try to take the kernel as $\boldsymbol{z}$ we do not get zero, because each z_i appears in two neighbouring terms that are positive. Hence the action for the (periodic) stadium billiard is piecewise strictly concave.

Acknowledgments

The author would like to thank Arnd Bäcker and Jim Meiss for illuminating discussions. This work was supported by the Deutsche Forschungsgemeinschaft.

References

[1] Poincaré H 1892 *Les Méthodes Nouvelles de la Mécanique Céleste* (Paris: Gauthier-Villars)
[2] Auerbach D *et al* 1987 *Phys. Rev. Lett.* **58** 2387
[3] Artuso R, Aurell E and Cvitanović P 1990 *Nonlinearity* **3** 325
[4] Gutzwiller M C 1990 *Chaos in Classical and Quantum Mechanics* (Berlin: Springer)
[5] Cvitanović P and Eckhardt B 1989 *Phys. Rev. Lett.* **63** 823
[6] Biham O and Wenzel W 1989 *Phys. Rev. Lett.* **63** 819
[7] Hansen K 1995 *Phys. Rev.* E **52** 2388
[8] Schmelcher P and Diakonos F K 1997 *Phys. Rev. Lett.* **78** 4733
[9] Percival I 1979 *Nonlinear Dynamics and the Beam–Beam Interaction* vol 57, ed M Month and J Herrera (New York: AIP)
[10] Aubry S and Daeron P L 1983 *Physica* **8D** 381
[11] Mather J 1982 *Topology* **21** 457
[12] Meiss J 1992 *Rev. Mod. Phys.* **64** 795
[13] Kook H and Meiss J 1989 *Physica* **35D** 65
[14] MacKay R and Meiss J 1992 *Nonlinearity* **5** 149
[15] Bunimovich L 1995 *Chaos* **5** 349
[16] Stojanov L 1989 *Commun. Math. Phys.* **124** 217
[17] Sieber M and Steiner F 1990 *Physica* **44D** 248
[18] Harayama T and Shudo A 1992 *J. Phys. A: Math. Gen.* **25** 4595
[19] Roberts A and Varberg D 1973 *Convex Functions* (New York: Academic)
[20] Bäcker A and Chernov N 1998 *Nonlinearity* **11** 79
[21] MacKay R and Meiss J 1983 *Phys. Lett.* **98A** 92
[22] Press W H, Flannery B P, Teukolsky S A and Vetterling W T 1988 *Numerical Recipes in C. The Art of Scientific Computing* (Cambridge: Cambridge University Press)
[23] Robnik M 1983 *J. Phys. A: Math. Gen.* **16** 3971
[24] Wojtkowski M P 1986 *Commun. Math. Phys.* **105** 391
[25] Bäcker A and Dullin H R 1997 *J. Phys. A: Math. Gen.* **30** 1991
[26] Bruus H and Whelan N D 1996 *Nonlinearity* **9** 1023
[27] Bunimovich L A 1979 *Commun. Math. Phys.* **65** 295
[28] Biham O and Kvale M 1992 *Phys. Rev.* A **46** 6334